Title
Ion exchange phenomena

Permalink
https://escholarship.org/uc/item/5p21m3r3

Author
Bourg, I.C.

Publication Date
2012

Ion Exchange Phenomena

Ian C. Bourg
Lawrence Berkeley National Laboratory

Garrison Sposito
University of California at Berkeley

This work was supported by the U.S. Department of Energy and LBNL under Contract No. DE-AC02-05CH11231.

6.1 Introduction

Ion exchange phenomena involve the population of *readily exchangeable ions*, the subset of adsorbed solutes that balance the intrinsic surface charge and can be readily replaced by major background electrolyte ions (Sposito, 2008). These phenomena have occupied a central place in soil chemistry research since Way (1850) first showed that potassium uptake by soils resulted in the release of an equal quantity of moles of charge of calcium and magnesium. Ion exchange phenomena are now routinely modeled in studies of soil formation (White et al., 2005), soil reclamation (Kopittke et al., 2006), soil fertilitization (Agbenin and Yakubu, 2006), colloidal dispersion/flocculation (Charlet and Tournassat, 2005), the mechanics of argillaceous media (Gajo and Loret, 2007), aquitard pore water chemistry (Tournassat et al., 2008), and groundwater (Timms and Hendry, 2007; McNab et al., 2009) and contaminant hydrology (Chatterjee et al., 2008; van Oploo et al., 2008; Serrano et al., 2009).

The prototypical chemical reaction equation for the exchange of cations A^{a+} and B^{b+} can be written as follows if X^- represents a mole of negative charge carried by the solid exchanger:

$$b\ X_aA_{(s)} + a\ B^{b+}{}_{(aq)} = a\ X_bB_{(s)} + b\ A^{a+}{}_{(aq)} \qquad (6.1)$$

Equation 6.1 can be modified in a straightforward manner to describe anion exchange reactions on positively charged surface sites. An example of Eq. 6.1 of importance to sodicity and the physical properties of soils is the heterovalent Na-Ca exchange reaction:

$$2\ \mathrm{XNa}_{(s)} + \mathrm{Ca}^{2+}{}_{(aq)} = \mathrm{X_2Ca}_{(s)} + 2\ \mathrm{Na}^{+}{}_{(aq)} \qquad (6.2)$$

Figure 6.1 shows an experimental *ion exchange isotherm* for the binary Na-Ca exchange reaction on a montmorillonitic soil (Fletcher and Sposito, 1984a), plotted as the fractional contribution of Ca^{2+} to the total adsorbed charge of exchangeable cations ($E_{\mathrm{Ca}} = q_{\mathrm{Ca}}/Q$, where $q_i = z_i n_i$ is the adsorbed charge of species i in $\mathrm{mol_c\ kg^{-1}}$ of solid, z_i and n_i being the valence of i and the moles of adsorbed i per kg solid, and $Q = \Sigma_i q_i$) against its fractional contribution to the charge concentration of all cations in solution [$\tilde{E}_{\mathrm{Ca}} = z_{\mathrm{Ca}} C_{\mathrm{Ca}}/\tilde{Q}$, where C_i is the molar concentration of species i ($\mathrm{mol\ dm^{-3}}$) and $\tilde{Q} = \Sigma z_i C_i$]. The convexity of the isotherm in Fig. 6.1 is typical of the competitive adsorption of the higher-valence ion in heterovalent exchange reactions. As shown below, however, this convexity does not imply selectivity or thermodynamic preference of the solid exchanger for Ca^{2+} vs. Na^{+}.

For practical applications, ion exchange isotherms are fitted with a variety of empirical one- or two-parameter models. The most widely used one-parameter models are those introduced by Vanselow, Gapon, and Gaines and Thomas:

$${}^{V}K_{A}{}^{B} = x_B{}^{a}/x_A{}^{b} \cdot (\mathrm{A}^{a+})^{b}/(\mathrm{B}^{b+})^{a} \qquad \text{(Vanselow, 1932)} \qquad (6.3)$$

$${}^{G}K_{A}{}^{B} = E_B/E_A \cdot (\mathrm{A}^{a+})^{1/a}/(\mathrm{B}^{b+})^{1/b} \qquad \text{(Gapon, 1933)} \qquad (6.4)$$

$${}^{GT}K_{A}{}^{B} = E_B{}^{a}/E_A{}^{b} \cdot (\mathrm{A}^{a+})^{b}/(\mathrm{B}^{b+})^{a} \qquad \text{(Gaines and Thomas, 1953)} \qquad (6.5)$$

where ${}^{V}K$, ${}^{G}K$ and ${}^{GT}K$ are the Vanselow, Gapon and Gaines-Thomas *selectivity coefficients*, (A^{a+}) is the thermodynamic activity of A^{a+} in aqueous solution, and x_A is the fractional contribution of A^{a+} to the total number of moles of exchangeable cations ($x_A = n_A/\Sigma_i n_i$). By definition, non-selective (or non-preference) Na-Ca binary exchange isotherms are obtained if

${}^{V}K = 1$, ${}^{G}K = 1$ or ${}^{GT}K = 1$; examples are plotted in Fig. 6.1 for $\tilde{Q} = 0.05$ (solid lines) and 0.5 mol dm^{-3} (dashed lines). Clearly, despite its name, non-selective exchange can differ among models and produce a strong, $\tilde{Q}$-dependent adsorption of the higher-valence ion; caution should therefore be used in assigning underlying mechanistic significance to isotherm shapes or selectivity coefficient values.

The most popular two-parameter model is the Rothmund-Kornfeld type model, on which the ratio of solute activities in Eqs. 6.3, 6.4 or 6.5 is raised to a fitted power n (Bond, 1995). The Rothmund-Kornfeld model based on Eq. 6.3, for example, is (Bond, 1995):

$$ {}^{VRK}K_A{}^{B} = x_B{}^{a}/x_A{}^{b} \cdot [(A^{a+})^{b}/(B^{b+})^{a}]^{n} \quad (6.6)$$

6.2 Surface charge and ion exchange capacities

As noted above, ion exchange phenomena involve adsorption reactions that balance the intrinsic surface charge of soil particles. The intrinsic surface charge density σ_{in} (mol$_c$ kg^{-1}) is the sum of the net structural surface charge density σ_0 (mol kg^{-1}) and the net proton surface charge density σ_H (mol kg^{-1}) (Sposito, 1998, 2008):

$$\sigma_{in} \equiv \sigma_0 + \sigma_H \quad (6.7)$$

The net structural ("permanent") surface charge density σ_0 results from crystalline defects such as isomorphic substitutions of Si$^{(IV)}$, Al$^{(III)}$ or Mg$^{(II)}$ by lower-valence cations in 2:1 phyllosilicates (smectites, vermiculites, illites and micas; Fig. 6.2a); for these 2:1 phyllosilicates, σ_0 contributes dominantly to σ_{in} and is invariably negative. The net proton ("variable") surface charge density σ_H [the difference between the moles of protons and the moles of hydroxide ions complexed by surface functional groups ($\sigma_H = q_H - q_{OH}$)] results from Brønsted acid surface groups with a pH-dependent charge, such as hydroxyl, carboxyl, or phenol groups (Fig. 6.2b); it is predominant in natural organic matter, kaolinite, and oxide minerals and can be negative, zero, or positive depending on pH, ionic strength, and other conditions.

Charge balance at solid-water interfaces imposes that Δq, the sum of the adsorbed ion charge densities q_i of all species except surface-complexed H^+ and OH^- ions, equals the opposite of the intrinsic surface charge density (Sposito, 1998, 2008):

$$\sigma_0 + \sigma_H + \Delta q = 0 \qquad (6.8)$$

The net adsorbed ion charge Δq can be expressed as a sum of the net charge of ions adsorbed in the Stern layer (σ_S) [ions immobile on time scales > 10 ps (Sposito et al., 1999)] or in the diffuse ion swarm (σ_d). The Stern layer charge component can be further divided into the contributions of inner-sphere (σ_{IS}) and outer-sphere (σ_{OS}) surface complexes (formed by direct contact of with surface functional groups or through one or more interposed water molecules, respectively) to yield the expression (Sposito, 1998, 2008):

$$\Delta q = \sigma_{IS} + \sigma_{OS} + \sigma_d \qquad (6.9)$$

The utility of Eq. 6.9 depends on the extent to which the molecular-scale coordination of adsorbed ions can be determined. Equation 6.7 and 6.8 show that σ_{in} and Δq can vary significantly with pH, ionic strength, and other variables that influence σ_H, especially in soils with low permanent structural charge (i.e., soils poor in 2:1 phyllosilicates). Experimental data on Δq vs. σ_H for a kaolinitic tropical soil suspended in LiCl solutions of varying ionic strength and pH (Fig. 6.3) confirm the inverse relationship between Δq and σ_H in Eq. 6.8 and the strong dependence of intrinsic surface charge density on experimental conditions. Thus, measured ion-exchange isotherms and *Q* values for such variable-charge soils may be highly sensitive to pH and other conditions that determine σ_H.

This pH-dependence of surface charge is characterized by points of zero charge, pH values at which one or more of the surface charge components in Eqs. 6.8 and 6.9 vanishes at fixed temperature, applied pressure, and aqueous solution composition (Sposito, 1998, 2008). For example, the pH value at which $\sigma_{in} = 0$ (where adsorbed cation and anion charge densities are equal according to Eqs. 6.7-6.8) is the point of zero net charge (p.z.n.c.). Nomenclature for these points of zero charge is listed in Table 6.2. Unfortunately, previous terminology for the points of zero charge has been highly erratic (for example, both the p.z.s.e. and the p.z.n.c. have been termed point of zero charge, while the p.z.n.p.c. has been termed zero point of charge). Furthermore, the points of zero charge frequently have been indirectly determined from experimental data on electrophoretic mobility or particle flocculation [calculations sensitive to the assumed distribution and mobility of ions in the electric double layer (Fair and Anderson, 1989; Hunter, 1993)], or from acid-base titrations of solid suspensions [calculations that often use untested assumptions on the initial value of the net proton surface charge (Sposito, 1998; Bourg et al., 2007)].

If all adsorbed ions (except surface-complexed H^+ and OH^-) are readily exchangeable, then Δq = CEC - AEC, where CEC is the cation exchange capacity [equal to Q plus the usually small positive equivalent adsorbed charge contributed by anion exclusion from the vicinity of X^- surface sites (Sposito, 2008)] and AEC is the anion exchange capacity (defined equivalently for anion exchange on positively charged surface functional groups). Ranges of the CEC of soils and soil constituents are listed in Table 6.1. The AEC of soils usually is less than 0.05 $mol_c\ kg^{-1}$ (Sposito, 2008). Major contributors to the CEC of soils are the widely-studied smectite clay minerals (Sposito et al., 1999; Sposito, 2008) and the less well-characterized soil organic matter (Helling et al., 1964; Curtin et al., 1998; Sutton and Sposito, 2005; Sposito, 2008). Micaceous minerals (illite, mica) also play an important role in the uptake of small quantities of weakly-solvated ions such as K^+, NH_4^+ and Cs^+ (Maes and Cremers, 1986; Bradbury and Baeyens, 2000).

6.3 Ion exchange thermodynamics

If Eq. 6.1 describes a true chemical equilibrium and the exchanger sites X^- are all identical (or are taken to represent an average site), a thermodynamic equilibrium constant or *exchange equilibrium coefficient* ${}^{ex}K$ can be defined with the relation (Sposito, 1994):

$$ {}^{ex}K_A{}^B = (X_bB)^a(A^{a+})^b / (X_aA)^b(B^{b+})^a \quad (6.10)$$

where (i) represents the thermodynamic activity of species i. The equilibrium constant ${}^{ex}K$ is directly related to the difference between the standard-state chemical potentials $\mu^0[\ldots]$ of the products and reactants in Eq. 6.1, termed the standard Gibbs energy change of the reaction: $\Delta_rG^0 = -RT \ln {}^{ex}K_A{}^B = a\mu^0[X_bB] + b\mu^0[A^{a+}] - b\mu^0[X_aA] - a\mu^0[B^{b+}]$, where R is the molar gas constant and T is absolute temperature.

The equilibrium chemical potentials μ of reactants and products typically differ from their standard-state values μ^0, and this difference must enter Eq. 6.10 through the thermodynamic activities on its right side. For the aqueous species A^{a+} and B^{b+}, the activity is defined by setting:

$$(i) \equiv \gamma_i\, C_i \qquad (6.11)$$

where γ_i is an activity coefficient (dm^{-3} mol), commonly expressed relative to the infinite dilution reference state at $T = 298.15$ K and $P = 1$ atm with the semi-empirical Davies equation (Sposito, 1994):

$$\ln \gamma_i = -0.512\, z_i^2\, \{\sqrt{I} / (1 + \sqrt{I}) - 0.3\, I\} \qquad (I < 0.5 \text{ mol dm}^{-3}) \qquad (6.12)$$

where I is the ionic strength ($I = 1/2\, \Sigma_i\, z_i^2 C_i$). For adsorbed species, if the exchanger phase is pictured as analogous to a solid solution of two components X_aA and X_bB, an appropriate model of thermodynamic activity should be (Argersinger et al., 1950; Sposito, 1994):

$$(i) \equiv f_i\, x_i \qquad (6.13)$$

where the rational activity coefficient f_i (dimensionless) is equal to 1 in the conventionally chosen reference state $x_i = 1$, $I = 0$, $T = 298.15$ K, and $P = 1$ atm (Gaines and Thomas, 1953; Sposito, 1994). No model for f_i of similar applicability and simplicity to Eq. 6.12 currently exists for f_i. However, Eqs. 6.3, 6.10, 6.13, and the Gibbs-Duhem relation at fixed T, P [$x_A \,\mathrm{dln} f_A + x_B \,\mathrm{dln} f_B = 0$] yield closed-form expressions for calculating ${}^{ex}K$ and f_i from experimental ion exchange isotherms at fixed $\tilde{Q}$ (Argersinger et al., 1950; Sposito, 1994):

$$\ln {}^{ex}K_A^B = \int_0^1 \ln {}^{V}K_A^B \cdot \mathrm{d}E_B \qquad (6.14)$$

$$b \ln f_A = E_B \ln {}^{V}K_A^B - \int_0^{E_B} \ln {}^{V}K_A^B \cdot \mathrm{d}E_B \quad (6.15)$$

In the context of the solid-solution picture, the A-B exchange is defined as *ideal* if $f_A = f_B = 1$, i.e. if ${}^{V}K_A{}^{B} = {}^{ex}K_A{}^{B}$, and *non-preference* if ${}^{ex}K_A{}^{B} = 1$. The Vanselow model in Eq. 6.3 therefore describes ideal binary exchange and the non-selective isotherms with ${}^{V}K = 1$ in Fig. 6.1 are *ideal thermodynamic non-preference isotherms*. Binary-exchange ${}^{ex}K$ values should obey the "triangle rule": $c \log {}^{ex}K_A{}^{B} + a \log {}^{ex}K_B{}^{C} + b \log {}^{ex}K_C{}^{A} = 0$, as has been verified within ± 0.1 log units for montmorillonite (Lewis and Thomas, 1963; Gast, 1969), vermiculite (Wild and Keay, 1964), and illite (Brouwer et al., 1983).

Since the reference state for surface species includes the ionic strength condition $I = 0$, Eqs. 6.14-6.15 are strictly valid only if applied to ${}^{V}K_A{}^{B}$ vs. E_B data measured at several $\tilde{Q}$ values and then extrapolated to $\tilde{Q} = 0$ (Gaines and Thomas, 1953). In practice, this extrapolation is rarely done, but ${}^{V}K$ values for exchange reactions on smectites and soils have been shown to have a rather small $\tilde{Q}$ -dependence (≤ 0.1 log units) if $\tilde{Q} \leq 0.2$ $\mathrm{mol_c\ dm^{-3}}$ (Laudelout et al., 1972; Jensen and Babcock, 1973). Furthermore, the rational activity coefficients f_i calculated with Eq. 6.15 are strictly valid only for the binary systems in which they were measured; expressions for f_i in ternary or more complex exchange systems are much more complicated (Chu and Sposito, 1981; Sposito, 1994). However, several models of comparable accuracy have been proposed for estimating ternary-system activity coefficients from binary ion exchange isotherm data (Bond and Verburg, 1997).

6.4 Trends in ^{V}K and ^{ex}K

Broad syntheses of ion exchange data for natural materials are scarce, despite the large number of reported experimental studies. This scarcity results in part from the complexity of soils. Even for smectite minerals (the most widely studied soil constituent) analyses of ion exchange data are complicated by the difficulty of isolating these clays [exchangeable cation homogenization and removal of carbonate, organic matter, and Al- and Fe-hydroxide impurities requires a careful choice of sample pretreatment and storage procedures (Duc et al., 2005)] and of accurately calculating the selectivity coefficient [^{V}K calculated without measuring C_i and q_i for all competing ions may be highly imprecise (Pabalan and Bertetti, 1999)]. In addition, the measured selectivity coefficients may vary with experimental conditions such as $\tilde{Q}$, pH, solid-liquid ratio m_s, or type of background anion because of poorly-understood processes such as ion-pair adsorption (Sposito et al., 1983a,b; Griffoen and Appelo, 1993; Charlet and Tournassat, 2005), adsorption on variable-charge sites on the edge surfaces of smectite lamellae (Fletcher and Sposito, 1989; Chen and Hayes, 1999), or the influence of experimental conditions on exchanger structure (Laird and Shang, 1997).

In the present section, we summarize current knowledge of the ion exchange selectivity of smectites, micaceous minerals, and soils based on reported ^{V}K and ^{ex}K values. In the case of smectites, we base our analysis as much as possible on studies that (1) used solid pretreatment practices known to produce pure, homoionic materials [a series of several acid washes (pH ≈ 4), exchangeable cation homogenization ($I \approx 1$ M), and rinsing steps followed by storage in liquid water at low temperature (Duc et al., 2005; Bourg et al., 2007)] and (2) measured q_i and C_i for all competing ions (Table 6.3). For the sake of brevity, we focus on results obtained at $T \approx 298$ K and do not discuss the temperature dependence of ${}^{V}K$ or the estimation of enthalpic and entropic contributions to the Gibbs energy of exchange (Gast, 1972; Maes and Cremers, 1978; Morel et al., 2007).

6.4.1 Smectites

Ion exchange reactions on smectites that involve only strongly-hydrated cations (Li^+, Na^+, and divalent metal cations M^{2+}) have ${}^{V}K$ values that display no hysteresis (Verburg and Baveye, 1994) and are independent of E_i within 0.1 log units (Gast, 1969; Sposito et al., 1981, 1983a,b,c; Suarez and Zahov, 1989; Tang and Sparks, 1993; Zhang and Sparks, 1996), i.e., they are *ideal* within experimental precision. [Erroneous reports of "non-ideal" heterovalent exchange reactions have been based on plots of ${}^{GT}K_A{}^B$ vs. E_B (Banin, 1968; Keren, 1979; McBride, 1980); e.g., the significant dependence of ${}^{GT}K_{Na}{}^M$ on E_M (M = Cu, Cu, Ni or Zn) observed for montmorillonite is in fact consistent with an ideal exchange reaction since ${}^{V}K_{Na}{}^M$ is independent of E_M (Sposito and Mattigod, 1979).] Exchange reactions between strongly hydrated cations are mildly selective (i.e., slightly favor the adsorption of cations of larger ionic radius or larger valence) and weakly affected by the type of smectite (Table 6.4). As expected from the near-ideality and weak selectivity of cation exchange reactions on smectites in the absence of weakly-hydrated ions, chemical speciation in such systems can be reasonably well described using $\log K_V \approx 0$ for all ion exchange reactions, e.g., the systems Na-H (Tournassat et al., 2004), Na-Cd, and Na-UO_2-$UO_2(OH)$-$(UO_2)_3(OH)_5$ (Zachara and McKinley, 1993).

Binary reactions that involve at least one weakly hydrated cation (K^+, NH_4^+, Rb^+, Cs^+, large organic cations, and, to a smaller extent, Ba^{2+}) are typically *non-ideal* and they frequently display hysteresis (Verburg and Baveye, 1994; Laird and Shang, 1997; Chatterjee et al., 1999) along with a strong dependence of ${}^{V}K$ on E_i (Gast, 1969; Maes and Cremers, 1978; McBride, 1979; Shainberg et al., 1987; Amrhein and Suarez, 1991), especially if the exchanging cations have very different hydration energies. This non-ideality may result in part [but not entirely (Maes and Cremers, 1978; Laird and Shang, 1997)] from the greater selectivity of *octahedral charge sites* vs. *tetrahedral charge sites* (i.e., sites resulting from isomorphic substitutions in the octahedral or tetrahedral sheet, respectively, of phyllosilicate minerals) for weakly hydrated cations (Xu and Harsh, 1992; Onodera et al., 2001). Among alkali metals and organic cations, the adsorption selectivity of weakly-hydrated cations increases with ionic radius (Gast, 1972; Maes and Cremers, 1986; Teppen and Aggarwal, 2007) because larger, less-strongly-hydrated ions have lower affinity for the aqueous solution phase (Mizutani et al., 1995; Teppen and Miller, 2006; Teppen and Aggarwal, 2007). Selectivity also increases with surface charge density (Gast, 1972; Maes and Cremers, 1978; Shainberg et al., 1987; Xu and Harsh, 1992) (Table 6.4) and perhaps especially with the charge density of octahedral charge sites (Xu and Harsh, 1992).

Metal-ligand complexes also can adsorb by ion exchange, but this process has not been deeply studied. The strong adsorption of copper-ethylenediamine complexes $Cu(en)_2^{2+}$ (Maes and Cremers, 1986) and the complexation of nitroaromatic compound with exchangeable cations on smectite surfaces (Chatterjee et al., 2008) are consistent with the expectation that metal-organic complexes should have an affinity similar to large organic cations for smectite surfaces. Divalent metals are known to co-adsorb with anions such as Cl^- (Sposito et al., 1983a,b; Charlet and Tournassat, 2005) or HCO_3^- (Griffoen and Appelo, 1993), but the mechanism of this co-adsorption (ion-pair formation or diffuse layer process) and its dependence on experimental conditions are not well understood (Sposito, 1991).

6.4.2 Micaceous minerals

Illites and micas have a lamellar morphology similar to that of smectites but with collapsed, K^+-filled interlayers (Sposito, 2008). The reactivity of external basal surfaces of illite and mica crystals is thought to be similar to that of smectites (Brouwer et al., 1983), but the crystals also carry a small population of sites (0.1-10 %) with a very high affinity for weakly-hydrated cations (K^+, NH_4^+, Rb^+, Cs^+) (Brouwer et al., 1983; Thellier and Sposito, 1989; Liu et al., 2004; Tournassat et al., 2007). These so-called *frayed-edge sites* occur at partially propped-open, K^+-depleted edges of collapsed interlayers (Rajec et al., 1999; McKinley et al., 2004). Adsorption on frayed-edge sites may be determined to a certain extent by non-equilibrium processes such as diffusion-controlled adsorption over time scales of weeks or more (Comans et al., 1991). Such processes can cause difficulties in defining and measuring ion exchange selectivity, since the population of "accessible" frayed-edge sites may vary with time, experimental conditions, the type of exchangeable cation, and the choice of agent used to extract adsorbed cations for measuring q_i (Brouwer et al., 1983; Comans et al., 1991; Baeyens and Bradbury, 2004; Tournassat et al., 2007). Nevertheless, the finding that frayed-edge sites obey the "triangle rule" (Brouwer et al., 1983) suggests that ion exchange on these sites can be reasonably well described on certain time scales as a thermodynamic process. If ion B = K, Rb or Cs, experimental ${}^{V}K_{A}^{B}$ values decrease sharply with E_B when the frayed-edge sites become B-saturated (Brouwer et al., 1983), a behavior that can be described with a two- or three-site model, i.e., one or two types of highly selective frayed-edge site plus weakly selective basal surface sites

(Maes and Cremers, 1986; Liu et al., 2004; Tournassat et al., 2007).

6.4.3 Soils and sediments

For highly heterogeneous, multiphase media such as soils and sediments, Eqs. 6.14-6.15 have no clear thermodynamic meaning and any selectivity model may be suitable on a case-by-case basis. For example, the Gapon selectivity coefficient has been found to be less variable than ^{V}K over broad ranges of exchanger phase composition for Na-Ca, Mg-K and Ca-K exchange reactions in some soils (Naylor and Overstreet, 1969; Jensen and Babcock, 1973; Evangelou and Coale, 1987; Feigenbaum et al., 1991; Agbenin and Yakubu, 2006). Experimental data on $\log{}^{V}K_{Ca}{}^{M}$ vs. E_M (M = Na, K or Mg) obtained for a range of conditions of pH, $\tilde{Q}$, and soil type illustrate the variability of the ion exchange selectivities of soils (Fig. 6.4). The scatter of $\log{}^{V}K_{Ca}{}^{Na}$ values at $E_{Na} \leq 0.2$ in Fig. 6.4b may reflect in part the high sensitivity of ^{V}K at small E_i values to sources of error such as the dissolution of soil materials (Carlson and Buchanan, 1973; Sheta et al., 1981).

Despite the inherent complexity of soil and sediment ion exchange properties, these have been modeled conceptually with some success assuming their exchange properties result from their smectite constituent (Charlet and Tournassat, 2005) or from the sum of their smectite, organic matter (Curtin et al., 1998), and/or micaceous constitutents (Bradbury and Baeyens, 2000). The first type of approximation is exemplified by the ion exchange properties of Amazon River suspended matter in the system Na-K-Ca-Mg, which are essentially identical to those of montmorillonite, even though only half of the CEC of the suspended matter originates from its clay size fraction (Charlet and Tournassat, 2005). The second type of approximation is well illustrated by the fact that the Mg-Ca exchange selectivity of soils is correlated with their ratio of organic carbon to clay content (Haghnia and Pratt, 1988; Curtin et al., 1998). Curtin et al. (1998)

successfully described the Mg-Ca selectivity of several soils with a two-site model where the soil organic matter and clay fractions were represented by log ${}^{V}K_{Mg}{}^{Ca}$ = 0.6 and 0.1, respectively. Similar additive behavior of soil smectites and soil organic matter has been used to interpret the ion exchange selectivity of montmorillonitic soils in the system Na-Ca-Mg (Fletcher et al., 1984b; Sposito and Fletcher, 1985) and also may explain the Ca-Sr selectivity of soils (Juo and Barber, 1969) and the Ca-Cd and Ca-Zn selectivity of acidic soils (Voegelin and Kretzchmar, 2003). Additive behavior of micaceous materials and other soil constituents may explain the strong adsorption of K^+ and Cs^+ at low E_K or E_{Cs} values in numerous soils and sediments (Feigenbaum et al., 1991; Bradbury and Baeyens, 2000; Sinanis et al., 2003; Liu et al., 2004; Agbenin and Yakubu, 2006). The concept that soil ion exchange selectivity is a sum of the selectivities of component phases evidently can be quite powerful (Sposito and Fletcher, 1985; Curtin et al., 1998; Bradbury and Baeyens, 2000; Charlet and Tournassat, 2005), although it neglects non-additive behavior such as the enhanced (about 0.3 log unit greater) Na-Ca selectivity of smectites when their interlayers contain Al-hydroxide polymers (Keren, 1979; Janssen et al., 2003).

6.5 Ion exchange and chemical speciation models

Analytical solutions of thermodynamic equations to determine exchanger phase composition rapidly become intractable in systems that involve more than three exchangeable ions (Bond and Verburg, 1997). For such complex systems, a numerical solution can be implemented in chemical speciation models after dividing Eq. 6.1 into two hypothetical half reactions involving a fictitious anionic species X^- (Sposito and Mattigod, 1977; Shaviv and Mattigod, 1985; Fletcher and Sposito, 1989):

$$\text{a } X^- + A^{a+}{}_{(aq)} = X_aA_{(s)} \quad (6.16a)$$

$$b\ X^- + B^{b+}_{(aq)} = X_bB_{(s)} \quad (6.16b)$$

Eq. 6.16 can be incorporated into conventional chemical speciation models by using its analogy with surface complexation or solid-solution reactions, as described below.

6.5.1 Modeling ion exchange as a surface complexation process

Most chemical speciation programs include a model of surface complexation reactions (similar in form to Eq. 6.16) where the thermodynamic activities of uncharged surface species arbitrarily are set equal to their concentrations $[X_i i]$ (Sposito, 2004). On this model, the half-reaction selectivity coefficients associated with Eq. 6.16 are the following (Fletcher and Sposito, 1989; Stadler and Schindler, 1993):

$$^{\text{half}}K^{A} = [X_aA] / (X^-)^a(A^{a+}) \qquad (6.17a)$$

$$^{\text{half}}K^{B} = [X_bB] / (X^-)^b(B^{b+}) \qquad (6.17b)$$

Equation 6.17 can be incorporated into any program that models surface complexation reactions; typically, $^{\text{half}}K$ is set to a very large value (10^{10}-10^{20}) for a reference cation, such that the wholly-uncomplexed X^- sites contribute negligibly to the total mass balance on X, and the $^{\text{half}}K$ values of other cations are chosen to fit experimental equilibrium constants (Flechter and Sposito, 1989; Stadler and Schindler, 1993). Certain chemical speciation programs include a specific model of ion-exchange reactions based on Eq. 6.17. For example, in the program PHREEQC2 (Appelo and Postma, 2005), the fictitious species X^- is excluded from the total mass balance on X and Na^+ is chosen as a reference species with log $^{\text{half}}K^{Na} = 0$. Suggested values of $^{\text{half}}K$ for other cations on smectite are provided in the PREEQC2 database (Appelo and Postma, 2005). The use of Eq. 6.17 with fixed $^{\text{half}}K$ values corresponds to an implicit assumption that $^{\text{GT}}K$ is equal to an equilibrium constant, since $^{\text{GT}}K$ and $^{\text{half}}K$ are related through:

$$^{\text{GT}}K_A{}^B = [(^{\text{half}}K^B)^a/(^{\text{half}}K^A)^b]\ (b^a/a^b)\ Q^{(b-a)} \qquad (6.18)$$

Equation 6.17 has been used to model ion exchange reactions involving protons, alkali metals, trace metals, and actinides on clay minerals (Stadler and Schindler, 1993; Zachara and McKinley, 1993; Turner et al., 1996; Poinssot et al., 1999; Bradbury and Baeyens 2000; Baeyens and Bradbury, 2004; Charlet and Tournassat, 2005; Heidmann et al., 2005; Bradbury and Baeyens, 2005, 2009; Bourg et al., 2007; Gu and Evans, 2008). Most of these studies [with the notable exception of Charlet and Tournassat (2005)] investigated systems where ${}^{\mathrm{half}}K$ should be constant if ion exchange is ideal, either because the main background electrolyte cation was $\mathrm{A}^{\mathrm{a}+}$ and occupied most ion exchange sites, such that ${}^{\mathrm{GT}}K_{\mathrm{A}}{}^{\mathrm{B}} \approx {}^{\mathrm{V}}K_{\mathrm{A}}{}^{\mathrm{B}}\ (\mathrm{b/a})^{\mathrm{a}}$, or because the system studied was homovalent, in which case ${}^{\mathrm{GT}}K_{\mathrm{A}}{}^{\mathrm{B}} = {}^{\mathrm{V}}K_{\mathrm{A}}{}^{\mathrm{B}}$.

6.5.2 Modeling ion exchange as a solid solution process

Some chemical speciation programs include a model of solid solution formation which also is similar in form to Eq. 6.16. The “solubility coefficients” associated with Eq. 6.16 are described as follows in the solid solution formalism (Appelo and Postma, 2005):

$$ {}^{\mathrm{solubility}}K^{\mathrm{A}} = (\mathrm{X}^-)^{\mathrm{a}}(\mathrm{A}^{\mathrm{a}+}) \,/\, x_{\mathrm{A}} f_{\mathrm{A}} \quad (6.19\mathrm{a}) $$

$$ {}^{\mathrm{solubility}}K^{\mathrm{B}} = (\mathrm{X}^-)^{\mathrm{b}}(\mathrm{B}^{\mathrm{b}+}) \,/\, x_{\mathrm{B}} f_{\mathrm{B}} \quad (6.19\mathrm{b}) $$

where (X^-) is the activity of a ficticious dissolved species. In the program PHREEQC2, Eq. 6.19 can be solved by defining X^-, $\mathrm{A}^{\mathrm{a}+}$ and $\mathrm{B}^{\mathrm{b}+}$ as dissolved species and $\mathrm{X_aA}$ and $\mathrm{X_bB}$ as solid phases and by setting ${}^{\mathrm{solubility}}K << 1$ for a chosen reference cation, such that X^- contributes negligibly to the mass balance on X [see the technical note by C.A.J. Appelo and D.L. Parkhurst, “Calculating cation exchange with PHREEQC (Version 2)” available at http://www.xs4all.nl/~appt/pub/ap_pa02.pdf]. If $f_{\mathrm{A}} = f_{\mathrm{B}} = 1$, Eq. 6.19 is identical to the Vanselov model with:

$$ {}^{\mathrm{V}}K_{\mathrm{A}}{}^{\mathrm{B}} = [({}^{\mathrm{solubility}}K^{\mathrm{B}})^{\mathrm{a}}/({}^{\mathrm{solubility}}K^{\mathrm{A}})^{\mathrm{b}}] \qquad (6.20) $$

The ideality of ion exchange reactions between strongly hydrated cations on smectite (Table 6.4) suggests that Eq. 6.19 may be more accurate than Eq. 6.17 for multicomponent ion exchange reactions on smectite over broad ranges of exchanger phase composition. However, to our knowledge, Eq. 6.19 has never been used for this purpose.

6.6 Micro- and nanoscale perspectives on ion exchange selectivity

Micro- and nanoscale studies have yielded insight into the processes that determine ${}^{V}K$ by using theoretical estimates of long-range electrostatic forces (Barak, 1989; Rytwo et al., 1996), short-range interactions (Shainberg and Kemper, 1966; Eberl, 1980), or statistical mechanical quantities (Sposito, 1993; Benjamin, 2002). In the present chapter, we focus on two subfields illustrating micro- and nanoscale studies: (1) the molecular-scale coordination and dynamics of exchangeable ions and (2) the influence of exchanger microstructure on ion exchange selectivity.

6.6.1 Molecular scale coordination and dynamics of exchangeable ions

Spectroscopic and molecular simulation methods have been widely used to probe the coordination environment and dynamics of exchangeable cations in smectites (Sposito and Prost, 1982; Sposito, 2004; Skipper et al., 2006) and have been increasingly applied to other exchanger phases (Skipper et al., 1995; Kim and Kirkpatrick, 1998; Schlegel et al., 2006; Xu et al., 2006). Spectroscopic techniques can probe the molecular structure of the interface as a function of distance from a solid surface [by x-ray reflectivity (Schlegel et al., 2006)], the dynamics of water H atoms [by quasi-elastic neutron scattering (QENS) (Marry et al., 2008)], the local coordination environment of certain atomic probes [such as water or Li by neutron diffraction with isotopic substitution (NDIS) (Skipper et al., 1995; Powell et al., 1998) or Co, Sr, Pb, Cu, Cs and other atoms by x-ray absorption spectroscopy (XAS) (Papelis and Hayes, 1996; Chen and Hayes, 1999; Strawn and Sparks, 1999; Morton et al., 2001; Bostick et al., 2002)], the coordination environment and rotational dynamics of paramagnetic atoms such as Cu [by electron spin resonance (ESR) or electron spin-echo modulation (ESEM) (McBride et al., 1975; Brown and Kevan, 1988)], and the local molecular environment ("chemical shielding") of atoms with an odd number of nucleons or protons such as ^{23}Na, ^{133}Cs, ^{113}Cd or ^{35}Cl [by nuclear magnetic resonance (NMR) (Weiss et al., 1990; Kim and Kirkpatrick, 1998; Xu et al., 2006)]. Molecular simulation techniques, primarily Monte Carlo (MC) and molecular dynamics (MD), have been used for over a decade to complement spectroscopic results (Chang et al., 1995; Park and Sposito, 2002). Most spectroscopic and simulation studies have been used to probe homoionic exchangers, but a few studies have investigated the behavior of a "reporter" cation doped into a smectite that is almost-homoionic in another cation (McBride et al., 1975; Brown and Kevan, 1988; Marry and Turq, 2003).

Spectroscopic and molecular simulation studies have shown that the aqueous phase in smectite interlayers is analogous to a concentrated ionic solution (Sposito and Prost, 1982; Powell et al., 1998); in the 2- and 3-layer hydrates and on external basal surfaces, it diffuses about 30 % as fast as bulk liquid water (Chang et al., 1997; Marry et al., 2008). Exchangeable cations in smectite 1-layer hydrates form inner-sphere surface complexes (ISSC) for obvious steric reasons and they diffuse very slowly (McBride et al., 1975; Chang et al., 1995, 1997); at higher hydration levels they can be divided into three categories based on their interaction with smectite surfaces: divalent metal cations (M^{2+}), strongly-hydrated alkali metal cations (Li^+, Na^+), and weakly-hydrated cations (K^+, Rb^+, Cs^+). The divalent cations are adsorbed in fully-solvated form as outer-sphere surface complexes (OSSC) or in the diffuse layer (DL) (McBride et al., 1975; Brown and Kevan, 1988; Papelis and Hayes, 1996; Chen and Hayes, 1999; Strawn and

Sparks, 1999; Greathouse et al., 2000; Morton et al., 2001; Chávez-Páez et al., 2001; Whitley and Smith, 2004); they tumble and diffuse slowly, about 1-10 % as fast as in bulk liquid water (McBride et al., 1975; Brown and Kevan, 1988; Greathouse et al., 2000). The strongly-hydrated monovalent cations (Li^+, Na^+) also adsorb as OSSC or DL species on octahedral charge sites, but they form inner-sphere surface complexes (ISSC) on tetrahedral charge sites (Chang et al., 1995, 1997; Leote de Carvalho and Skipper, 2001; Marry and Turq, 2003; Marry et al., 2003; Greathouse and Cygan, 2005; Tambach et al., 2004, 2006); they diffuse about 30-60 % as fast as in bulk water if adsorbed on octahedral charge sites, but are essentially immobile (on sub-nanosecond time scales) on tetrahedral charge sites (Chang et al., 1995, 1997; Leote de Carvalho and Skipper, 2001; Marry and Turq, 2003). Finally, the weakly-hydrated cations form primarily ISSC on smectite surfaces along with small amounts of OSSC or DL species (Chang et al., 1998; Nakano et al., 2003; Whitley and Smith, 2004; Tambach et al., 2006; Liu et al., 2008); two populations of ISSC exist in Cs- and K-smectite interlayers that may correspond to cations located above ditrigonal cavities or "triads" of O atoms of the siloxane surface (Weiss et al., 1990; Onodera et al., 2001; Park and Sposito, 2002; Nakano et al., 2003); the mobility of these cations along smectite basal surfaces is not well characterized (Kosakowski et al., 2008). Clearly, the molecular-scale behavior of cations on smectites parallels their ion exchange selectivity: the strongly-hydrated cations (M^{2+}, Li^+, Na^+) adsorb mainly as fully solvated OSSC or DL species and display ideal, weakly-selective ion exchange behavior, whereas the weakly-hydrated ions adsorb mainly as ISSC and display non-ideal, strongly-selective ion exchange behavior. The ISSC formed by Li^+ and Na^+ on tetrahedral charge sites do not fit this simple classification, suggesting that Li^+ and Na^+ may show non-ideal exchange behavior on smectites with high tetrahedral charge. This point may not have been noticed previously because reference smectites typically carry 80 ± 20 % octahedral charge sites (Xu and Harsh, 1992).

Thanks to increases in computational capabilities, MD and MC simulations may soon be able to “bridge the gap” from the time and length scales (or number of MC simulation steps) required to probe molecular exchanger phase structure and dynamics (< 1 ns and ≤ 1 nm) to the time and length scales (10-100 ns and 10-100 nm) on which ion exchange equilibria become established (Greathouse and Cygan, 2005; Rotenberg et al., 2007). Molecular simulation methods could then be used to test Eq. 6.13 directly or to predict ${}^{V}K$ values (Greathouse and Cygan, 2005; Teppen and Miller, 2006). Teppen and Miller (2006) showed that the Gibbs energy difference between K-, Rb-, and Cs-montmorillonite (one component of the Gibbs energy of exchange) at fixed interlayer spacing and interlayer water content could be determined by MD simulation. Greathouse and Cygan (2005) found that ten 1-ns MD simulations of a 4-nm-thick Na^{+}-UO_2^{2+}-CO_3^{2-} aqueous solution on a montmorillonite basal surface were too short and small-scale to determine ${}^{V}K$ accurately, but were sufficient to identify important processes, such as the formation of $[Na_2UO_2(CO_3)_3]^{2-}$ complexes.

6.6.2 Coupling between cation exchange and exchanger structure

As pointed out above, Eq. 6.10 has strict thermodynamic meaning only if all exchanger sites X^- are identical. For smectites (Sposito, 1992; Laird and Shang, 1997) and natural organic matter (Sutton et al., 2005), however, the microstructure of the exchanger phase depends on experimental conditions and, therefore, the X^- may *not* be identical at different points along a binary exchange isotherm, or even in different regions of the exchanger phase within a single sample. In the case of smectite clay minerals, the stacking arrangement of smectite lamellae (number of layers per stack, interlayer spacing) is a dynamic, non-uniform property [several interlayer hydration levels may coexist (Tamura et al., 2000; Wilson et al., 2004; Ferrage et al., 2005)] that depends on the magnitude and location of clay structural charge (Slade et al., 1991; Tambach et al., 2004), the population of adsorbed cations (Schramm and Kwak, 1982; Sposito, 1992; Laird and Shang, 1997; Ferrage et al., 2005) (Table 6.5), the thermodynamic activity of water (Norrish, 1954; Slade et al., 1991; Laird et al., 1995), as well as the previous history of the clay (Verburg and Baveye, 1994; Laird et al., 1995; Chatterjee et al., 2008) and its degree of compaction (Kozaki et al., 1998). Molecular-scale simulations confirm that homoionic montmorillonites frequently exhibit several stable states of crystalline swelling separated by energy barriers (Whitley and Smith, 2004; Tambach et al., 2004, 2006; Smith et al., 2006). Transitions between these states are predominantly enthalpic (Whitley and Smith, 2004), driven by cationic solvation energy (Whitley and Smith, 2004)—as opposed to being determined by the hydrogen bond network of interlayer water (Tambach et al., 2006)—strongly hysteretic (Tambach et al., 2006), and in fact thermodynamically analogous to a phase transition (Laird and Shang, 1997; Whitley and Smith, 2004).

The stacking arrangement, in turn, determines the fraction of X^- sites located on external vs. internal basal surfaces, which may have unequal cation exchange selectivities (Keren, 1979; Sposito et al., 1983a), and the fraction of internal-surface X^- sites in contact with 1-, 2- or 3-layer interlayer hydrates, which also may have unequal cation exchange selectivities (Barak, 1989; Laird and Shang, 1997; Van Loon and Glaus, 2008). Thus cation exchange on swelling clay minerals involves a feedback loop among adsorption, exchanger structure, and selectivity (Laird and Shang, 1997; Fig. 6.4) that is reminiscent of the behavior of certain ion-selective pores (Kuyucak et al., 2001). This feedback loop may explain the occurrence of exchangeable cation "de-mixing" (Shainberg and Otoh, 1968; Fink et al., 1971; Iwasaki and Watanabe, 1988), increased selectivity for the preferred cation at high surface loading of the same cation

(Shainberg et al., 1980; Laird and Shang, 1997, Janssen et al., 2003), cation exchange hysteresis (Fripiat et al., 1965; Verburg et al., 1995), and increased selectivity for weakly-hydrated ions as smectite charge density increases (Maes and Cremers, 1978; Shainberg et al., 1987). Smectite ^{ex}K values would then have thermodynamic meaning only if defined for a certain particle arrangement (Laird and Shang, 1997). Thus the non-ideality of cation exchange reactions that involve weakly-hydrated cations may be related to the fact that these cations cause a sequential collapse of the interlayer from a 3-layer hydrate or more (for Li^+, Na^+, and strongly hydrated divalent cations M^{2+}) to a 2-layer hydrate (for K^+ and Ba^{2+}) to a 1-layer hydrate (for Cs^+) (Table 6.5).

6.7 Bibliographic References

Agbenin J.O. and Yakubu S., 2006. Potassium-calcium and potassium-magnesium exchange equilibria in an acid savanna soil from northern Nigeria. Geoderma 136, 542-554.

Amrhein C. and Suarez D.L., 1991. Sodium-calcium exchange with anion exclusion and weathering corrections. Soil Sci. Soc. Am. J. 55, 698-706.

Appelo C.A.J. and Postma D., 2005. Geochemistry, Groundwater and Pollution, 2nd Ed., Balkema Publ., New York.

Argersinger W.J., Jr., Davidson A.W. and Bonner O.D., 1950. Thermodynamics and ion exchange phenomena. Trans. Kans. Acad. Sci. 53, 404-410.

Baeyens B. and Bradbury M.H., 2004. Cation exchange capacity measurements on illite using the sodium and cesium isotope dilution technique: Effects of the index cation, electrolyte concentration and competition: Modeling. Clays Clay Miner. 52, 421-431.

Banin A., 1968. Ion exchange isotherms of montmorillonite and structure factors affecting them. Isr. J. Chem. 6, 27-36.

Barak P., 1989. Double layer theory prediction of Al-Ca exchange on clay and soil. J. Colloid Interface Sci. 133, 479-490.

Benjamin M.M., 2002. Modeling the mass-action expression for bidentate adsorption. Environ. Sci. Technol. 36, 307-313.

Bond W.J., 1995. On the Rothmund-Kornfeld description of cation exchange. Soil Sci. Soc. Am. J. 59, 436-443.

Bond W.J. and Verburg K., 1997. Comparison of methods for predicting ternary exchange from binary isotherms. Soil Sci. Soc. Am. J. 61, 444-454.

Bostick B.C., Vairavmurthy M.A., Karthikeyan K.G. and Chorover J., 2002. Cesium adsorption on clay minerals: An EXAFS spectroscopic investigation. Environ. Sci. Technol. 36, 2670 2676.

Bourg I.C., Sposito G. and Bourg A.C.M., 2007. Modeling the acid-base surface chemistry of montmorillonite. J. Colloid Interface Sci. 312, 297-310.

Bradbury M.H. and Baeyens B., 2000. A generalized sorption model for the concentration dependent uptake of caesium by argillaceous rocks. J. Contam. Hydrol. 42, 141-163.

Bradbury M.H. and Baeyens B., 2005. Modelling the sorption of Mn(II), Co(II), Ni(II), Zn(II), Cd(II), Eu(III), Am(III), Sn(IV), Th(IV), Np(V) and U(VI) on montmorillonite: Linear free energy relationships and estimates of surface binding constants for some selected heavy metals and actinides. Geochim. Cosmochim. Acta 69, 875-892.

Bradbury M.H. and Baeyens B., 2009. Sorption modelling on illite Part I: Titration measurements and the sorption of Ni, Co, Eu and Sn. Geochim. Cosmochim. Acta 73, 990-1003.

Brouwer E., Baeyens B., Maes A. and Cremers A., 1983. Cesium and rubidium ion equilibria in illite clay. J. Phys. Chem. 87, 1213-1219.

Brown D.R. and Kevan L., 1988. Aqueous coordination and location of exchangeable Cu^{2+} cations in montmorillonite clay studied by electron spin resonance and electron spin-echo modulation. J. Am. Chem. Soc. 110, 2743-2748.

Carlson R.M. and Buchanan J.R., 1973. Calcium-magnesium-potassium equilibria in some California soils. Soil Sci. Soc. Am. Proc. 37, 851-855.

Chang F.-R.C., Skipper N.T. and Sposito G., 1995. Computer simulation of interlayer molecular structure in sodium montmorillonite hydrates. Langmuir 11, 2734-2741.

Chang F.-R.C., Skipper N.T. and Sposito G., 1997. Monte Carlo and molecular dynamics simulations of interfacial structure in lithium-montmorillonite hydrates. Langmuir 13, 2074-2082.

Chang F.-R.C., Skipper N.T. and Sposito G., 1998. Monte Carlo and molecular dynamics simulations of electrical double-layer structure in potassium montmorillonite hydrates. Langmuir 14, 1201-1207.

Charlet L. and Tournassat C., 2005. Fe(II)-Na(I)-Ca(II) cation exchange on montmorillonite in chloride medium: Evidence for preferential clay adsorption of chloride – metal ion pairs in seawater. Aquatic Geochem. 11, 115-137.

Chatterjee R., Laird D.A. and Thompson M.L., 2008. Interactions among K^{+}-Ca^{2+} exchange, sorption of m-dinitrobenzene, and smectite quasicrystal dynamics. Environ. Sci. Technol. 42, 9099-9103.

Chávez-Páez M., de Pablo L. and de Pablo J.J., 2001. Monte Carlo simulations of Ca-montmorillonite hydrates. J. Chem. Phys. 114, 10948-10953.

Chen C.-C. and Hayes K.F., 1999. X-ray absorption spectroscopy investigation of aqueous

Co(II) and Sr(II) sorption at clay-water interfaces. Geochim. Cosmochim. Acta 63, 3205-3215.

Chorover J. and Sposito G., 1995. Surface charge characteristics of kaolinitic tropical soils. Geochim. Cosmochim. Acta 59, 875-884.

Chu S.-Y. and Sposito G., 1981. The thermodynamics of ternary cation exchange systems and the subregular model. Soil Sci. Soc. Am. J. 45, 1084-1089.

Comans R.N.J., Haller M. and de Preter P., 1991. Sorption of cesium on illite: Non-equilibrium behaviour and reversibility. Geochim. Cosmochim. Acta 55, 433-440.

Curtin D., Selles F. and Steppuhn H., 1998. Estimating calcium-magnesium selectivity in smectititc soils from organic matter and texture. Soil Sci. Soc. Am. J. 62, 1280-1285.

DeSutter T.M., Pierzynski G.M. and Baker L.R., 2006. Flow-through and batch methods for determining calcium-magnesium and magnesium-calcium selectivity. Soil Sci. Soc. Am. J. 70, 550-554.

Duc M., Gaboriaud F. and Thomas F., 2005. Sensitivity of the acid-base properties of clays to the methods of preparation and measurement. 1. Literature review. J. Colloid Interface Sci. 289, 139-147.

Eberl D.D., 1980. Alkali cation selectivity and fixation by clay minerals. Clays Clay Miner. 28, 161-172.

Evangelou V.P. and Coale F.J., 1987. Dependence of the Gapon coefficient on exchangeable sodium for mineralogically different soils. Soil Sci. Soc. Am. J. 51, 68-72.

Fair M.C. and Anderson J.L., 1989. Electrophoresis of nonuniformly charged ellipsoidal particles. J. Colloid Interface Sci. 127, 388-400.

Feigenbaum S., Bar-Tal A., Portnoy R. and Sparks D.L., 1991. Binary and ternary exchange of potassium on calcareous montmorillonitic soils. Soil Sci. Soc. Am. J. 55, 49-56.

Ferrage E., Tournassat C., Rinnert E. and Lanson B., 2005. Influence of pH on the interlayer cationic composition and hydration state of Ca-montmorillonite: Analytical chemistry, chemical modelling and XRD profile modelling study. Geochim. Cosmochim. Acta 69, 2797-2812.

Fink D.H., Nakayama F.S. and McNeal B.L., 1971. Demixing of exchangeable cations in free-swelling bentonite clay. Soil Sci. Soc. Am. Proc. 35, 552-555.

Fletcher P., Sposito G. and LeVesque C.S., 1984a. Sodium-calcium-magnesium exchange reactions on a montmorillonitic soil: I. Binary exchange reactions. Soil Sci. Soc. Am. J. 48, 1016-1021.

Fletcher P., Holtzclaw K.M., Jouany C., Sposito G. and LeVesque C.S., 1984b. Sodium-calcium-magnesium exchange reactions on a montmorillonitic soil: II. Ternary exchange reactions. Soil Sci. Soc. Am. J. 48, 1022-1025.

Fletcher P. and Sposito G., 1989. The chemical modelling of clay/electrolyte interactions for montmorillonite. Clay Miner. 24, 375-391.

Fripiat J.J., Cloos P. and Poncelet A., 1965. Comparaison entre les propriétés d’échange de la montmorillonite et d’une résine vis-à-vis des cations alcalins et alcalino-terreux. I. Réversibilité des processus. Bull. Soc. Chim. Fr. 1, 208-215.

Gaines G.L. and Thomas H.C., 1953. Adsorption studies on clay minerals. II. A formulation of the thermodynamics of exchange adsorption. J. Chem. Phys. 21, 714-718.

Gajo A. and Loret B., 2007. The mechanics of active clays circulated by salts, acids and bases. J. Mech. Phys. Solids 55, 1762-1801.

Gapon, Ye.N., 1933. On the theory of exchange adsorption in soils. J. Gen. Chem. USSR

(Engl. Trans.) 3, 144-160, cited by Sposito and Mattigod (1977).

Gast R.G., 1969. Standard free energies of exchange for alkali metal cations on Wyoming bentonite. Soil Sci. Soc. Am. J. 33, 37-41.

Gast R.G., 1972. Alkali metal cation exchange on Chambers montmorillonite. Soil Sci. Soc. Am. 36, 14-19.

Greathouse J.A., Refson K. and Sposito G., 2000. Molecular dynamics simulation of water mobility in magnesium-smectite hydrates. J. Am. Chem. Soc. 122, 11459-11464.

Greathouse J.A. and Cygan R.T., 2005. Molecular dynamics simulation of uranyl(VI) adsorption equilibria onto an external montmorillonite surface. Phys. Chem. Chem. Phys. 7, 3580-3586.

Griffoen J. and Appelo C.A.J., 1993. Adsorption of calcium and its complexes by two sediments in calcium-hydrogen-chlorine-carbon dioxide systems. Soil Sci. Soc. Am. J. 57, 716-722.

Gu X. and Evans L.J., 2008. Surface complexation modelling of Cd(II), Cu(II), Ni(II), Pb(II) and Zn(II) adsorption onto kaolinite. Geochim. Cosmochim. Acta 72, 267-276.

Heidmann I., Christl I., Leu C. and Kretzschmar R., 2005. Competitive sorption of protons and metal cations onto kaolinite: experiments and modeling. J. Colloid Interface Sci. 282, 270-282.

Helling C.S., Chesters G. and Corey R.B., 1964. Contribution of organic matter and clay to soil cation-exchange capacity as affected by the pH of the saturating solution. Soil Sci. Soc. Am. Proc. 28, 517-520.

Hunter R.J., 1993. Introduction to Modern Colloid Science. Oxford University Press, Oxford.

Iwasaki T. and Watanabe T., 1988. Distribution of Ca and Na ions in dioctahedral smectites and interstratified dioctahedral mica/smectites. Clays Clay Miner. 36, 73-82.

Janssen R.P.T., Bruggenwert M.G.M. and van Riemsdijk W.H., 2003. Effect of Al hydroxide polymers on cation exchange of montmorillonite. Europ. J. Soil Sci. 54, 335-345.

Jensen H.E. and Babcock K.L., 1973. Cation-exchange equilibria on a Yolo loam. Hilgardia 41, 475-487.

Juo A.S.R. and Barber S.A., 1969. An explanation for the variability in Sr-Ca exchange selectivity of soils, clays and humic acid. Soil Sci. Soc. Am. Proc. 33, 360-363.

Keren R., 1979. The effect of hydroxy-aluminum precipitation on the exchange properties of montmorillonite. Clays Clay Miner. 27, 303-304.

Kim Y. and Kirkpatrick R.J., 1998. NMR T_1 relaxation study of ^{133}Cs and ^{23}Na adsorbed on illite. Amer. Mineral. 83, 661-665.

Kopittke P.M., So H.B. and Menzies N.W., 2006. Effect of ionic strength and clay mineralogy on Na-Ca exchange and the SAR-ESP relationship. Europ. J. Soil Sci. 57, 626-633.

Kosakowski G., Churakov S.V. and Thoenen T., 2008. Diffusion of Na and Cs in montmorillonite. Clays Clay Miner. 56, 190-206.

Kozaki T., Fujishima A., Sato S. and Ohashi H., 1998. Self-diffusion of sodium ions in compacted sodium montmorillonite. Nucl. Technol. 121, 63-69.

Kuyucak S., Andersen O.S. and Chung S.-H., 2001. Models of permeation in ion channels. Rep. Prog. Phys. 64, 1427-1472.

Laird D.A., Shang C. and Thompson M.L., 1995. Hysteresis in crystalline swelling of smectites. J. Colloid Interface Sci. 171, 240-245.

Laird D.A. and Shang C., 1997. Relationship between cation exchange selectivity and crystalline swelling in expanding 2:1 phyllosilicates. Clays Clay Miner. 45, 681-689.

Laudelout H., van Bladel R. and Robeyns J., 1972. Hydration of cations adsorbed on a clay surface from the effect of water activity on ion-exchange selectivity. Soil Sci. Soc. Am. Proc. 36, 30-34.

Leote de Carvalho R.J.F. and Skipper N.T., 2001. Atomistic computer simulation of the clay-fluid interface in colloidal laponite. J. Chem. Phys. 114, 3727-3733.

Levy G.J., van der Watt H.v.H., Shainberg I. and du Plessis H.M., 1988. Potassium-calcium and sodium calcium exchange on kaolinite and kaolinitic soils. Soil Sci. Soc. Am. J. 52, 1259-1264.

Lewis R.J. and Thomas H.C., 1963. Adsorption studies on clay minerals. VIII. A consistency test of exchange sorption in the systems sodium-cesium-barium montmorillonite. J. Phys. Chem. 67, 1781-1783.

Liu C., Zachara J.M. and Smith S.C., 2004. A cation exchange model to describe Cs^+ sorption at high ionic strength in subsurface sediments at Hanford site, USA. J. Contam. Hydrol. 68, 217-238.

Liu X., Lu X., Wang R. and Zhou H., 2008. Effects of layer-charge distribution on the thermodynamic and microscopic properties of Cs-smectite. Geochim. Cosmochim. Acta 72, 1837-1847.

Maes A. and Cremers A., 1977. Charge density effects in ion exchange. Part 1. Heterovalent exchange equilibria. J. Chem. Soc., Faraday Trans. I 73, 1807-1814.

Maes A. and Cremers A., 1978. Charge density effects in ion exchange. Part 2. Homovalent exchange equilibria. J. Chem. Soc., Faraday Trans. I 74, 1234-1241.

Maes A. and Cremers A., 1986. Highly selective ion exchange in clay minerals and zeolites. In: Geochemical Processes at Mineral Surfaces (Davis J.A. and Hayes K.F., Eds.) American Chemical Society, Washington, DC, pp. 254-295.

Marry V. and Turq P., 2003. Microscopic simulations of interlayer structure and dynamics in bihydrated heteroionic montmorillonites. J. Phys. Chem. B 107, 1832-1839.

Marry V., Dufreche J.F., Jardat M., Meriguet G., Turq P. and Grun F., 2003. Dynamics and transport in charged porous media. Colloids Surf. A 222, 147-153.

Marry V., Malikova N., Cadène A., Dubois E., Durand-Vidal S., Turq P., Breu J., Longeville S. and Zanotti J.-M., 2008. Water diffusion in a synthetic hectorite by neutron scattering—beyond the isotropic translational model. J. Phys.: Condens. Matter 20, 104205.

McBride M.B., Pinnavaia T.J. and Mortland M.M., 1975. Electron spin resonance studies of cation orientation in restricted water layers on phyllosilicate (smectite) surfaces. J. Phys. Chem. 79, 2430-2435.

McBride M.B., 1979. An interpretation of cation selectivity variations in M^+-M^+ exchange on clays. Clays Clay Miner. 27, 417-422.

McBride M.B., 1980. Interpretation of the variability of selectivity coefficients for exchange between ions of unequal charge on smectites. Clays Clay Miner. 28, 255-261.

McKinley J.P., Zachara J.M., Heald S.M., Dohnalkova A., Newville M.G. and Sutton S.R., 2004. Microscale distribution of cesium sorbed to biotite and muscovite. Environ. Sci. Technol. 38, 1017-1023.

McNab W.W., Jr., Singleton M.J., Moran J.E. and Esser B.K., 2009. Ion exchange and trace element surface complexation reactions associated with applied recharge of low-TDS water in the San Joaquin Valley, California. Appl. Geochem. 24, 129-137.

Mizutani T., Takano T. and Ogoshi H., 1995. Selectivity of adsorption of organic ammonium ions onto smectite clays. Langmuir 11, 880-884.

Morel J.-P., Marry V., Turq P. and Morel-Desrosiers N., 2007. Effect of temperature on the retention of Cs^+ by Na-montmorillonite: microcalorimetric investigation. J. Mater. Chem. 17, 2812-2817.

Morton J.D., Semrau J.D. and Hayes K.F., 2001. An X-ray absorption spectroscopy study of the structure and reversibility of copper adsorbed to montmorillonite clay. Geochim. Cosmochim. Acta 65, 2709-2722.

Nakano M., Kawamura K. and Ichikawa Y., 2003. Local structural information of Cs in smectite hydrates by means of an EXAFS study and molecular dynamics simulations. Appl. Clay Sci. 23, 15-23.

Naylor D.V. and Overstreet R., 1969. Sodium-calcium exchange behavior in organic soils. Soil Sci. Soc. Am. Proc. 33, 848-851.

Norrish K., 1954. Manner of swelling of montmorillonite. Nature 173, 256-257.

Onodera Y., Iwasaki T., Ebina T., Hayashi H., Torii K., Chatterjee A. and Mimura H., 1998. Effect of layer charge on fixation of cesium ions in smectites. J. Contam. Hydrol. 35, 131-140.

Pabalan R.T. and Bertetti F.P., 1999. Experimental and modeling study of ion exchange between aqueous solutions and the zeolite mineral clinoptilolite. J. Solution Chem. 28, 367-393.

Papelis C. and Hayes K.F., 1996. Distinguishing between interlayer and external sorption sites of clay minerals using X-ray absorption spectroscopy. Colloids Surf. A 107, 89-96.

Park S.-H. and Sposito G., 2002. Structure of water adsorbed on a mica surface. Phys. Rev. Lett. 89, 085501.

Poinssot C., Baeyens B. and Bradbury M.H., 1999. Experimental and modeling studies of caesium sorption on illite. Geochim. Cosmochim. Acta 63, 3217-3227.

Powell D.H., Fischer H.E. and Skipper N.T., 1998. The structure of interlayer water in Li-montmorillonite studied by neutron diffraction with isotopic substitution. J. Phys. Chem. B 102, 10899-10905.

Rajec P., Sucha V., Eberl D.D., Srodon J. and Elsass F., 1999. Effect of illite particle shape on cesium sorption. Clays Clay Miner. 47, 755-760.

Rhue R.D. and Mansell R.S., 1988. The effect of pH on sodium-calcium and potassium-calcium exchange selectivity for Cecil soil. Soil Sci. Soc. Am. J. 52, 641-647.

Rotenberg B., Marry V., Vuilleumier R., Malikova N., Simon C. and Turq P., 2007. Water and ions in clays: Unraveling the interlayer/micropore exchange using molecular dynamics. Geochim. Cosmochim. Acta 71, 5089-5101.

Rytwo G., Banin A. and Nir S., 1996. Exchange reactions in the Ca-Mg-Na-montmorillonite system. Clays Clay Miner. 44, 276-285.

Schlegel M.L., Nagy K.L., Fenter P., Cheng L., Sturchio N.C. and Jacobsen S.D., 2006. Cation sorption on the muscovite (001) surface in chloride solutions using high-resolution X-ray reflectivity. Geochim. Cosmochim. Acta 70, 3549-3565.

Schramm L.L. and Kwak J.C.T., 1982. Influence of exchangeable cation composition on the size and shape of montmorillonite particles in dilute suspension. Clays Clay Miner. 30, 40-48.

Serrano S., O'Day P.A., Vlassopoulos D., García-González M.T. and Garrido F., 2009. A surface complexation and ion exchange model of Pb and Cd competitive sorption on natural soils. Geochim. Cosmochim. Acta 73, 543-558.

Shainberg I. and Kemper W.D., 1966. Hydration status of adsorbed cations. Soil Sci. Soc. Am. Proc. 30, 707-713.

Shainberg I. and Otoh H., 1968. Size and shape of montmorillonite particles saturated with Na/Ca ions (inferred from viscosity and optical measurements). Isr. J. Chem. 6, 251-259.

Shainberg I., Oster J.D. and Wood J.D., 1980. Sodium/calcium exchange in montmorillonite and illite suspension. Soil Sci. Soc. Am. J. 44, 960-964.

Shainberg I., Alperovitch N.I. and Keren R., 1987. Charge density and Na-K-Ca exchange on smectites. Clays Clay Miner. 35, 68-73.

Shaviv A. and Mattigod S.V., 1985. Cation exchange equilibria in soils expressed as cation-ligand complex formation. Soil Sci. Soc. Am. J. 49, 569-573.

Sheta T.H., Gobran G.R., Dufey J.E. and Laudelout H., 1981. Sodium-calcium exchange in Nile delta soils: Single values for Vanselow and Gaines-Thomas selectivity coefficients. Soil Sci. Soc. Am. J. 45, 749-753.

Sinanis C., Keramidas V.Z. and Sakellariadis S., 2003. Thermodynamics of potassium-magnesium exchange in two Alfisols of northern Greece. Comm. Soil Sci. Plant Anal. 34, 439-456.

Skipper N.T., Smalley M.V., Williams G.D., Soper A.K. and Thompson C.H., 1995. Direct measurement of the electric double-layer structure in hydrated lithium vermiculite clays by neutron diffraction. J. Phys. Chem. 99, 14201-24204.

Skipper N.T., Lock P.A., Titiloye J.O., Swenson J., Mirza Z.A., Howells W.S. and Fernandez-Alonso F., 2006. The structure and dynamics of 2-dimensional fluids in swelling clays. Chem. Geol. 230, 182-196.

Slade P.G., Quirk J.P. and Norrish K., 1991. Crystalline swelling of smectite samples in concentrated NaCl solutions in relation to layer charge. Clays Clay Miner. 39, 234-238.

Smith D.E., Wang Y., Chaturvedi A. and Whitley H.D., 2006. Molecular simulations of the pressure, temperature, and chemical potential dependencies of clay swelling. J. Phys. Chem. B 110, 20046-20054.

Sposito G. and Mattigod S. V., 1977. On the chemical foundation of the sodium adsorption ratio. Soil Sci. Soc. Am. J. 41, 323-329.

Sposito G. and Mattigod S.V., 1979. Ideal behavior in Na-trace metal cation exchange on Camp Bertaux montmorillonite. Clays Clay Miner. 27, 125-128.

Sposito G., Holtzclaw K.M., Johnston C.T. and LeVesque C.S., 1981. Thermodynamics of sodium-copper exchange on Wyoming bentonite at 298 K. Soil Sci. Soc. Am. J. 45, 1079-1084.

Sposito G. and Prost R., 1982. Structure of water adsorbed on smectites. Chem. Rev. 82, 553-573.

Sposito G., Holtzclaw K.M., Charlet L., Jouany C. and Page A.L., 1983a. Sodium-calcium and sodium-magnesium exchange on Wyoming bentonite in perchlorate and chloride background ionic media. Soil Sci. Soc. Am. J. 47, 51-56.

Sposito G., Holtzclaw K.M., Jouany C. and Charlet L., 1983b. Cation selectivity in sodium-calcium, sodium-magnesium and calcium-magnesium exchange on Wyoming bentonite at 298 K. Soil Sci. Soc. Am. J. 47, 917-921.

Sposito G., Jouany C., Holtzclaw K.M. and LeVesque C.S., 1983c. Calcium-magnesium exchange on Wyoming bentonite in the presence of adsorbed sodium. Soil Sci. Soc. Am.

J. 47, 1081-1085.

Sposito G. and Fletcher P., 1985. Sodium-calcium-magnesium exchange reactions on a montmorillonitic soil: III. Calcium-magnesium exchange selectivity. Soil Sci. Soc. Am. J. 49, 1160-1163.

Sposito G., 1991. Effect of chloride ions on sodium-calcium and sodium-magnesium exchange on montmorillonite. Soil Sci. Soc. Am. J. 55, 965-967.

Sposito G., 1992. The diffuse-ion swarm near smectite particles suspended in 1:1 electrolyte solutions: modified Gouy-Chapman theory and quasicrystal formation. In: Clay-Water Interface and its Rheological Implications (N. Güven and R.M. Pollastro, Eds.), The Clay Minerals Society, Boulder, CO, pp. 128-155.

Sposito G., 1993. Surface complexation of metals by natural colloids. In: Ion Exchange and Solvent Extraction, Vol. II. (J.A. Marinsky and Y. Marcus, Eds.), Marcel Dekker, New York, pp. 211-236.

Sposito G., 1994. Chemical Equilibria and Kinetics in Soils, Oxford University Press, Oxford.

Sposito G., 1998. On points of zero charge. Environ. Sci. Technol. 32, 2815-2819.

Sposito G., Skipper N.T., Sutton R., Park S.-H., Soper A.K. and Greathouse J.A., 1999. Surface geochemistry of the clay minerals. Proc. Natl. Acad. Sci. USA 96, 3358-3364.

Sposito G., 2004. The Surface Chemistry of Natural Particles, Oxford University Press, Oxford.

Sposito G., 2008. The Surface Chemistry of Soils, 2nd. Ed., Oxford University Press, Oxford.

Stadler M. and Schindler P.W., 1993. Modeling of H^+ and Cu^{2+} adsorption on calcium-montmorillonite. Clays Clay Miner. 41, 288-296.

Strawn D.G. and Sparks D.L., 1999. The use of XAFS to distinguish between inner- and outer-sphere lead adsorption complexes on montmorillonite. J. Colloid Interface Sci. 216, 257-269.

Sutton R. and Sposito G., 2005. Molecular structure in soil humic substances: The new view. Environ. Sci. Technol. 39, 9009-9015.

Sutton R., Sposito G., Diallo M.S. and Schulten H.-R., 2005. Molecular simulation of a model of dissolved organic matter. Environ. Toxicol. Chem. 24, 1902-1911.

Tambach T.J., Hensen E.J.M. and Smit B.J., 2004. Molecular simulations of swelling clay minerals. J. Phys. Chem. B 108, 7586-7596.

Tambach T.J., Bolhuis P.G., Hensen E.J.M. and Smit B., 2006. Hysteresis in clay swelling induced by hydrogen bonding: Accurate prediction of swelling states. Langmuir 22, 1223-1234.

Tamura K., Yamada H. and Nakazawa H., 2000. Stepwise hydration of high-quality synthetic smectite with various cations. Clays Clay Miner. 48, 400-404.

Tang L. and Sparks D.L., 1993. Cation-exchange kinetics on montmorillonite using pressure-jump relaxation. Soil Sci. Soc. Am. J. 57, 42-46.

Teppen B.J. and Miller D.M., 2006. Hydration energy determines isovalent cation exchange selectivity by clay minerals. Soil Sci. Soc. Am. J. 70, 31-40.

Teppen B.J. and Aggarwal V., 2007. Thermodynamics of organic cation exchange selectivity in smectites. Clays Clay Miner. 55, 119-130.

Thellier C. and Sposito G., 1989. Influence of electrolyte concentration on quaternary cation exchange by Silver Hill illite. Soil Sci. Soc. Am. J. 53, 705-711.

Timms W.A. and Hendry M.J., 2007. Quantifying the impact of cation exchange on longterm solute transport in a clay-rich aquitard. J. Hydrol. 332, 110-122.

Tournassat C., Ferrage E., Poinsignon C. and Charlet L., 2004. The titration of clay minerals. Part II. Structural-based model and implications for clay reactivity. J. Colloid Interface Sci. 273, 234-246.

Tournassat C., Gailhanou H., Crouzet C., Braibant G., Gautier A., Lassin A., Blanc P. and Gaucher E.C., 2007. Two cation exchange models for direct and inverse modelling of solution major cation composition in equilibrium with illite surfaces. Geochim. Cosmochim. Acta 71, 1098-1114.

Tournassat C., Lerouge C., Blanc P., Brendlé J., Greneche J.-M., Touzelet S. and Gaucher E.C., 2008. Cation exchanged Fe(II) and Sr compared to other divalent cations (Ca, Mg) in the bure Callovian-Oxfordian formation: Implications for porewater composition modelling. Appl. Geochem. 23, 641-654.

Van Bladel R. and Gheyi H.R., 1980. Thermodynamic study of calcium-sodium and calcium-magnesium exchange in calcareous soils. Soil Sci. Soc. Am. J. 44, 938-942.

Van Loon L.R. and Glaus M.A., 2008. Mechanical compaction of smectite clays increases ion exchange selectivity for cesium. Environ. Sci. Technol. 42, 1600-1604.

van Oploo P., White I., Ford P., Melville M.D. and Macdonald B.C.T., 2008. Pore water chemistry of acid sulfate soils: Chemical flux and oxidation rates. Geoderma 146, 32-39.

Vanselow A.P., 1932. Equilibria of the base-exchange reactions of bentonites, permutities, soil colloids, and zeolites. Soil Sci. 33, 95-113.

Verburg K. and Baveye P., 1994. Hysteresis in the binary exchange of cations on 2:1 clay minerals: A critical review. Clays Clay Miner. 42, 207-220.

Verburg K., Baveye P. and McBride M.B., 1995. Cation-exchange hysteresis and dynamics of formation and breakdown of montmorillonite quasi-crystals. Soil Sci. Soc. Am. J. 59, 1268-1273.

Voegelin A. and Kretzschmar R., 2003. Modelling sorption and mobility of cadmium and zinc in soils with scaled exchange coefficients. Europ. J. Soil Sci. 54, 387-400.

Way J.T., 1850. On the power of soils to absorb manure. J. Roy. Agr. Soc. Engl. 11, 313-379.

Weiss C.A., Jr., Kirkpatrick R.J. and Altaner S.P., 1990. The structural environments of cations adsorbed onto clays: ^{133}Cs variable-temperature MAS NMR spectroscopic study of hectorite. Geochim. Cosmochim. Acta 54, 1655-1669.

White A.F., Schulz M.S., Vivit D.V., Blum A.E., Stonestrom D.A. and Harden J.W., 2005. Chemical weathering rates of a soil chronosequence on granitic alluvium: III. Hydrochemical evolution and contemporary solute fluxes and rates. Geochim. Cosmochim. Acta 69, 1975-1996.

Whitley H.D. and Smith D.E., 2004. Free energy, energy, and entropy of swelling in Cs-, Na-, and Sr-montmorillonite clays. J. Chem. Phys. 120, 5387-5395.

Wild A. and Keay J., 1964. Cation exchange equilibria with vermiculite. J. Soil Sci. 15, 135-144.

Wilson J., Cuadros J., and Cressey G., 2004. An in situ time-resolved XRD-PSD investigation into Na-montmorillonite interlayer and particle rearrangement during dehydration. Clays Clay Miner. 52, 180-191.

Xu S. and Harsh J.B., 1992. Alkali cation selectivity and surface charge of 2:1 clay minerals. Clays Clay Miner. 40, 567-574.

Xu X., Kalinichev A.G. and Kirkpatrick R.J., 2006. ^{133}Cs and ^{35}Cl NMR spectroscopy and molecular dynamics modeling of Cs^+ and Cl^- complexation with natural organic matter. Geochim. Cosmochim. Acta 70, 4319-4331.

Zachara J.M. and McKinley J.P., 1993. Influence of hydrolysis on the sorption of metal cations by smectites: Importance of edge coordination reactions. Aquatic Sci. 55, 250-261.

Zhang Z.Z. and Sparks D.L., 1996. Sodium-copper exchange on Wyoming montmorillonite in chloride, perchlorate, nitrate, and sulfate solutions. Soil Sci. Soc. Am. J. 60, 1750-1757.

Table 6.1 Typical cation exchange capacities (CEC, in $\text{mol}_c\ \text{kg}^{-1}$) of soils and major soil constituents, based primarily on Sposito (2004, 2008).

Solid	CEC
soils	0.01-1.4
Natural organic matter	0.8-10[a]
Vermiculite	1.6-2.5
Smectite	0.7-1.7
Illite	0.2
Mica	0.1
Kaolinite	< 0.05

[a] Increasing with pH and in the order peat < humic acid.

Table 6.2 Points of zero charge.

Symbol	Name	Definition
p.z.n.c.	point of zero net charge	$\sigma_{in} = 0$
p.z.n.p.c.	point of zero net proton charge	$\sigma_H = 0$
p.z.c.	point of zero charge	$\sigma_p = 0$[a]
p.z.s.e.	point of zero salt effect	$\partial\sigma_H/\partial I = 0$

[a] σ_p ($\equiv \sigma_0 + \sigma_H + \sigma_{IS} + \sigma_{OS}$) is the net particle surface charge density.

Table 6.3 Compilation of the best available data sets on cation exchange on smectite clay minerals. The studies by Gast (1972) and Maes and Cremers (1977, 1978) are tentatively included, despite the fact that they did not include measurements of q_i values, because of the good quality of their pre-treatment methods. Studies that used smectites stored by freeze-drying also are tentatively included although storage in liquid water at low temperature is preferred (Duc et al., 2005). Experimental procedures that may adversely affect the quality of experimental results are reported in italics in the last column.

Reference	Solid	Cations	Comments
Gast (1972)	Arizona montmorillonite	Na-Li, Na-K, Na-Rb, Na-Cs	$\tilde{Q}$ = 1 mmol$_c$ dm^{-3} (Cl$^-$ electrolyte); T = 298 K; *m_s not specified*; *q_i values not measured.*
Maes and Cremers (1977)	Otay and RCCB[a] montmorillonites	Na-Ca	$\tilde{Q}$ = 10 mmol$_c$ dm^{-3} (Cl$^-$ electrolyte); T = 298 K; $m_s \approx$ 10 g kg^{-1}; *q_i values not measured.*
Maes and Cremers (1978)	Otay and RCCB montmorillonites, hectorite	Na-Cs	$\tilde{Q}$ = 10 mmol dm^{-3} (Cl$^-$ electrolyte); T = 298 K; *m_s not specified*; pH = 5.5-6; *clay stored in freeze-dried form*; *q_i values not measured.*
Sposito et al. (1981)	Wyoming montmorillonite	Na-Cu	$\tilde{Q}$ = 10 mmol$_c$ dm^{-3} (Cl$^-$ or ClO$_4^-$ electrolytes); T = 298 K; m_s = 13-21 g kg^{-1}; pH = 5-6 to avoid Cu adsorption on oxide-type edge surface sites.
Sposito et al. (1983a,b,c)	Wyoming montmorillonite	Na-Ca, Na-Mg, Ca-Mg, Na-Ca-Mg	$\tilde{Q}$ = 50 mmol$_c$ dm^{-3} (Cl$^-$ or ClO$_4^-$ electrolytes); T = 298 K; m_s = 20-30 g kg^{-1}; pH = 6.8-7.1.
Xu and Harsh (1992)	Cameron montmorillonite	Na-Li, Na-K, Na-Rb, Na-Cs	$\tilde{Q}$ = 10 mmol$_c$ dm^{-3} (Cl$^-$ electrolyte); T = 298 K; *m_s not specified*; c_i and q_i values not reported; *^VK values reported only at E_{Na} = 0.5.*
Tang and Sparks (1993)	Wyoming montmorillonite	Na-Ca, K-Ca	I = 10 mmol dm^{-3} (Cl$^-$ electrolyte); T = 296 K; m_s = 10.2 g dm^{-3}; pH = 6.8; *clay stored in freeze-dried form.*
Zhang and Sparks (1996)	Wyoming montmorillonite	Na-Cu	$\tilde{Q}$ = 20 mmol$_c$ dm^{-3} (ClO$_4^-$, Cl$^-$, NO$_3^-$ or SO$_4^{2-}$ electrolyte); T = 298 K; $m_s \approx$ 16-17 g dm^{-3}; *pH = 5.2 to 6.5, decreasing as q_{Cu} increases*; *clay*

			stored in freeze-dried form.
Laird and Shang (1997)	Synthetic fluoro-hectorite	Mg-Ba	$\tilde{Q}$ = 20 mmol$_c$ dm^{-3} (Cl$^-$ electrolyte); T = room temperature; m_s = 10 g dm^{-3}; no acid wash, but the material is a synthetic magnesium silicate so should not contain Al or Fe hydroxides or organic impurities; *clay stored in freeze-dried form*.
Charlet and Tournassat (2005)	Wyoming montmorillonite	Na-Fe(II), Ca-Fe(II), Na-Ca-Fe(II)	$\tilde{Q}$ = 50 or 130 mmol$_c$ dm^{-3} (Cl$^-$ electrolyte); T *not specified*; m_s = 4-8 g dm^{-3}; pH = 2.1-3.6 to avoid Fe adsorption on oxide-type edge surface sites; q_{Fe} *not measured (estimated by mass balance)*.

[a] RCCB montmorillonite: reduced-charge Camp-Berteau (Morocco) montmorillonite. Layer charge was reduced by 5 to 41 % using the Hofmann-Klemen effect (Maes and Cremers, 1977, 1978).

Table 6.4 Recommended values for ${}^{V}K$ on smectite based on the studies listed in Table 6.3 (confidence intervals calculated as ± 2σ where several ${}^{V}K$ values were available).

Variable	log *K*	References
Exchanges of two strongly hydrated cations		
${}^{V}K_{Na}{}^{Li}$	-0.08 ± 0.06	Gast (1972), Xu and Harsh (1992)
${}^{V}K_{Na}{}^{M(II)}$	0.11 ± 0.11[a] (M = Mg, Ca, Cu)	Maes and Cremers (1977), Sposito et al. (1981,1983a), Tang and Sparks (1993), Zhang and Sparks (1996)
${}^{V}K_{Mg}{}^{Ca}$	0.01 ± 0.02 (E_{Na} = 0, 0.016 or 0.036)	Sposito et al. (1983b,c)
${}^{V}K_{Fe(II)}{}^{Ca}$	~0.01	Charlet and Tournassat (2005)[b]
Exchanges involving at least one weakly hydrated cation		
${}^{ex}K_{Na}{}^{K}$	0.58 ± 0.14[c]	Gast (1972), Xu and Harsh (1992)
${}^{ex}K_{Na}{}^{Rb}$	1.08 ± 0.25[c]	Gast (1972), Xu and Harsh (1992)
${}^{ex}K_{Na}{}^{Cs}$	1.23 × CEC – 0.06[d]	Gast (1972), Maes and Cremers (1978), Xu and Harsh (1992)
${}^{V}K_{Mg}{}^{Ba}$	~0.5 in the 3-layer hydrate, increasing to ~1.4 in the 2-layer hydrate	Laird and Shang (1997)

[a] Neglecting Na-Ca exchange data obtained with reduced-charge montmorillonites, which show ${}^{V}K_{Na}{}^{Ca}$ values closer to zero (Maes and Cremers, 1977).

[b] Charlet and Tournassat (2005) erroneously reported their ${}^{GT}K$ values as ${}^{V}K$ values, but for homoionic Ca-Fe(II) exchange ${}^{GT}K = {}^{V}K$.

[c] log ${}^{ex}K_{Na}{}^{K}$ and log ${}^{ex}K_{Na}{}^{Rb}$ are thought to increase with *Q* (Shainberg et al., 1987; Xu and Harsh, 1992).

[d] Linear regression with $r^2 = 0.91$, $p < 0.001$; CEC = 0.66 to 1.44 $mol_c\ kg^{-1}$, estimated from the number of octahedral and tetrahedral substitutions in the clay unit cell formula.

Table 6.5 Interlayer hydration level (Norrish, 1954; Laird and Shang, 1997; Chatterjee et al., 2008) and number of lamellae per stack (Sposito, 1992; Verburg and Baveye, 1994; Verburg et al., 1995) in dilute aqueous suspensions of homoionic montmorillonite.

Cation	Hydration level[a]	Lamellae per stack
Li^+	> 3	1.0
Na^+	> 3	1.0-1.7
K^+	2	1.0-7.0
Cs^+	1-2	1.4-4.0
Mg^{2+}	3	2.7-14.0
Ca^{2+}	3	3.0-20.0
Ba^{2+}	2-3	2.7-7.0

[a] Number of statistical water monolayers in each smectite interlayer.

Figure 6.1 Binary Na-Ca ion exchange isotherm on a montmorillonitic soil at $\tilde{Q} = 0.05$ mol$_c$ dm^{-3} [diamonds, Fletcher and Sposito (1984a)] plotted as E_{Ca} vs. $\tilde{E}_{Ca}$. Non-selective isotherms were calculated for the Vanselow (thick lines) and Gapon conventions (thin lines) at $\tilde{Q} = 0.05$ and 0.5 mol dm^{-3} (solid lines and dashed lines, respectively).

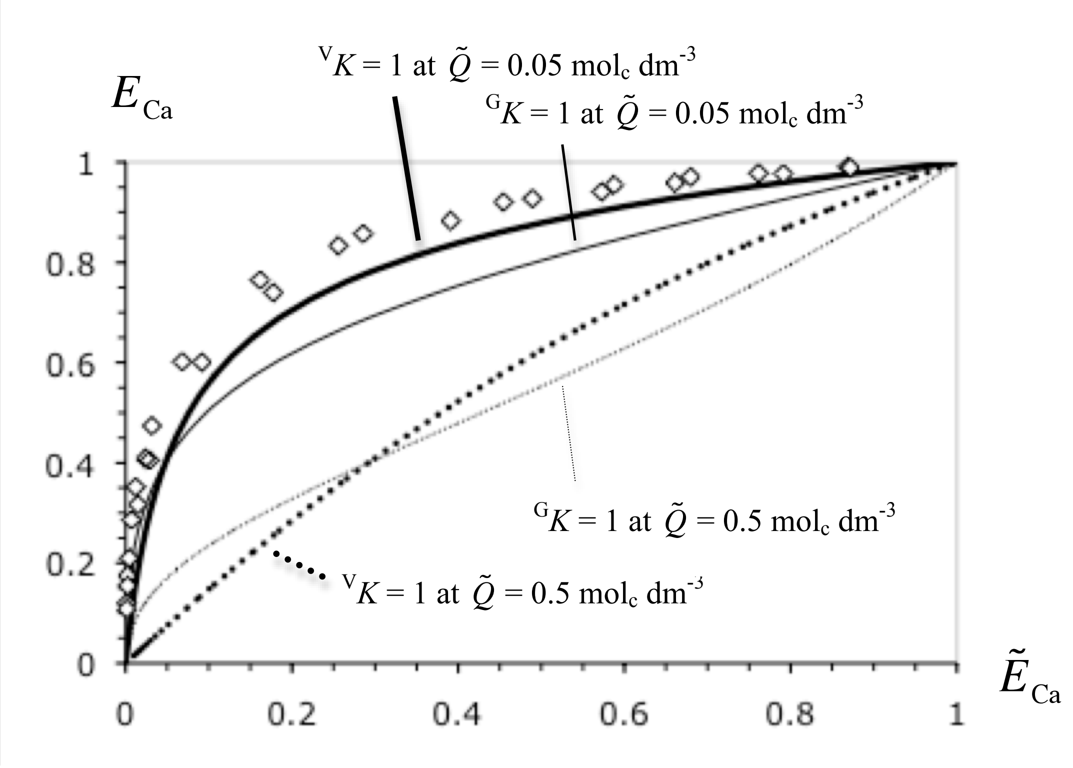

Figure 6.2 Major types of ion exchange sites in natural materials: (a) clay siloxane surfaces located near a site of isomorphic substitution [shown only as the basal surface O atoms (red) and tetrahedral sheet Si atoms (gray) of two stacked smectite lamellae with a K^+ ion (black, forming an inner-sphere surface complex) and nearby water molecules in the interlayer space (Sposito et al., 1999)]; (b) pH-dependent sites resulting from the deprotonation of Lewis acid groups on organic matter or mineral oxide surfaces [here three carboxyl groups of natural organic matter (with C atoms in gray) coordinating an almost completely desolvated Ca^{2+} ion in dark red (Sutton et al., 2005)].

a.

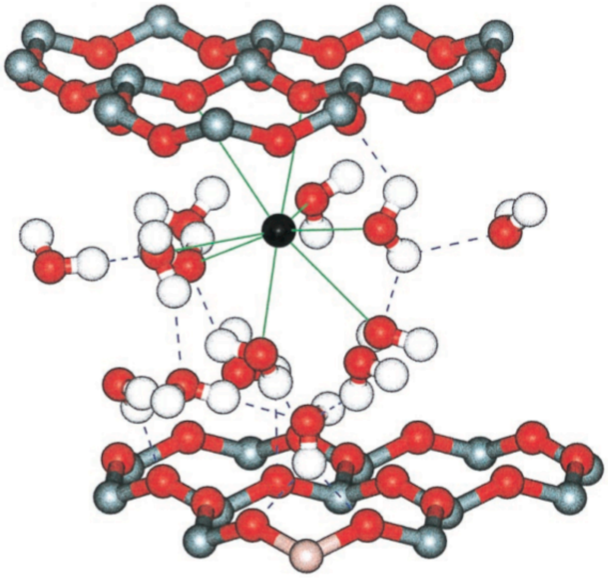

b.

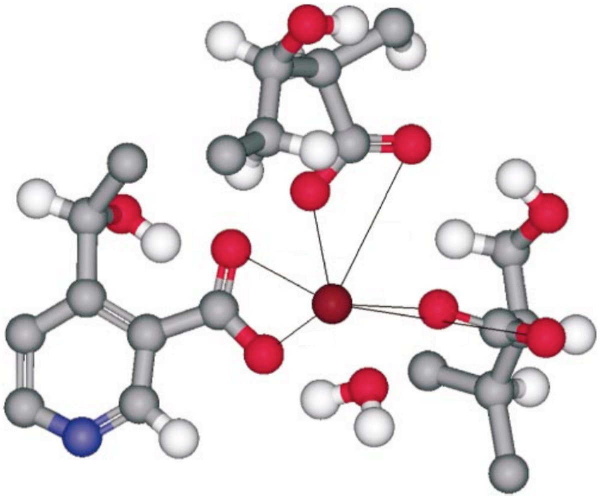

Figure 6.3 "Chorover plot" (Chorover and Sposito, 1995) of the net adsorbed ion charge against the net proton surface charge density for a Brazilian Oxisol (Manaus soil). The combined data, for ionic strengths of 0.001 (open circles), 0.005 (crosses), and 0.01 (filled circles) mol kg^{-1}, can be fit to the regression equation (solid line): $\Delta q = -1.01(\pm 0.07)\sigma_H + 12.5(\pm 0.8)$, where Δq and σ_H are in $mmol_c\ kg^{-1}$. Charge balance is confirmed by the values of the slope and both intercepts ($\sigma_0 = 12.5 \pm 0.4\ mmol_c\ kg^{-1}$ in direct measurement).

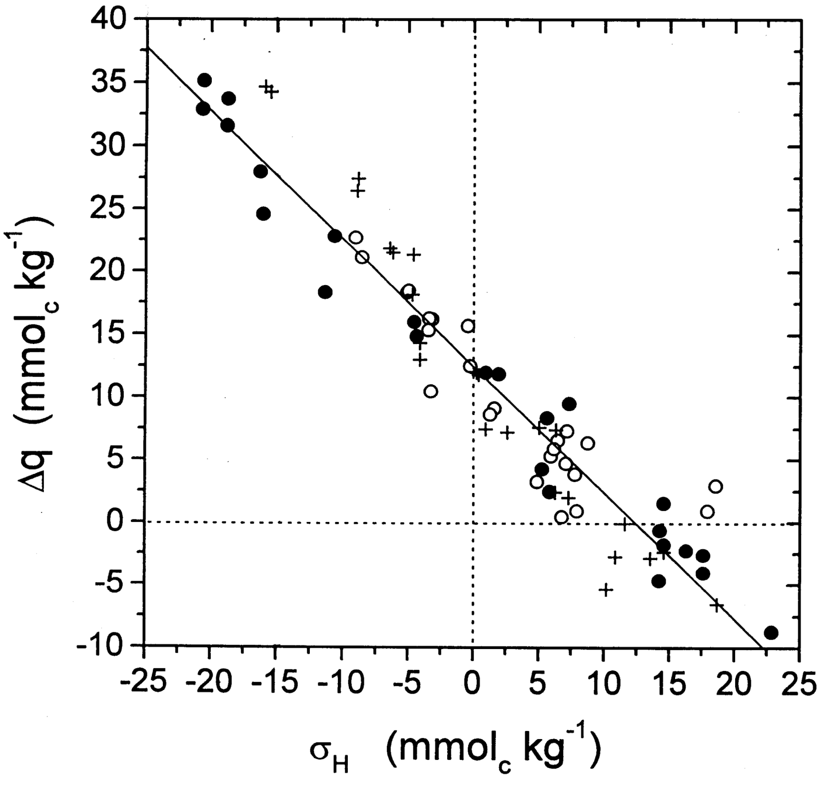

Figure 6.4 Compilation of experimental data on $\log{}^{V}K_{Ca}^{M}$ vs. E_M (M = Mg^{2+}, Na^+ or K^+) in soils if $\tilde{Q} \leq 0.2$ mol dm^{-3} and $T = 298$ K; (a) $\log{}^{V}K_{Ca}^{Mg}$ data for a loam soil (Jensen and Babcock, 1973), calcareous clay soils (Van Bladel and Gheyi, 1980), smectitic soils with 27 to 96 g kg^{-1} organic carbon (Curtin et al., 1998), and a montmorillonitic soil (DeSutter et al., 2006); (b) $\log{}^{V}K_{Ca}^{Na}$ for a montmorillonitic soil (Fletcher et al., 1984a), kaolinitic soils (Levy et al., 1988), a kaolinitic sandy loam soil with 25.7 g kg^{-1} organic carbon (Rhue and Mansell, 1988), a calcareous, smectitic clay soil (Amrhein and Suarez, 1991), and an illite-kaolinite clay soil (Bond, 1995); (c) $\log{}^{V}K_{Ca}^{K}$ for a loam soil (Jensen and Babcock, 1973), kaolinitic soils (Levy et al., 1988), a kaolinitic sandy loam soil with 25.7 g kg^{-1} organic carbon (Rhue and Mansell, 1988), an illite-kaolinite clay soil (Bond, 1995), and a tropical soil (Agbenin and Yakubu, 2006).

a.

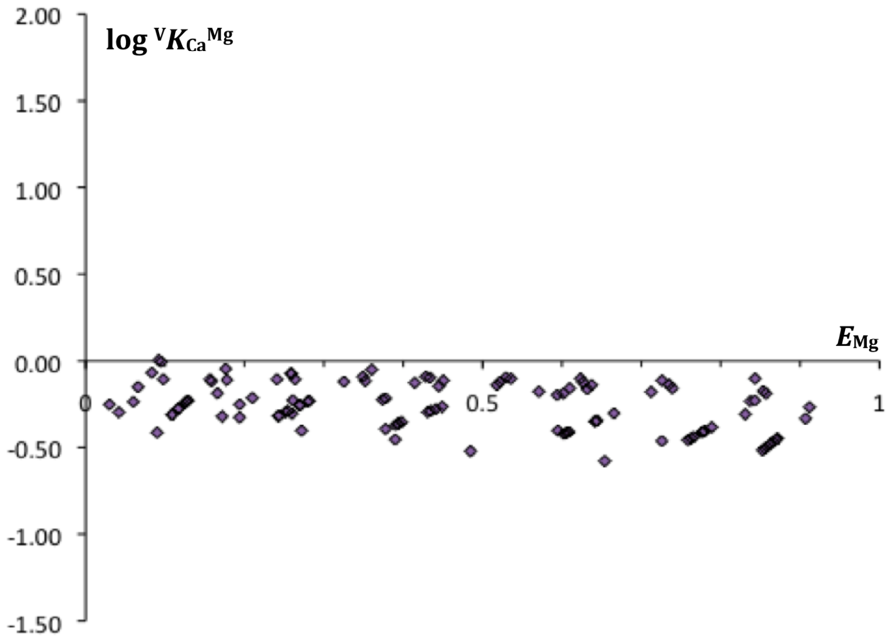

b.

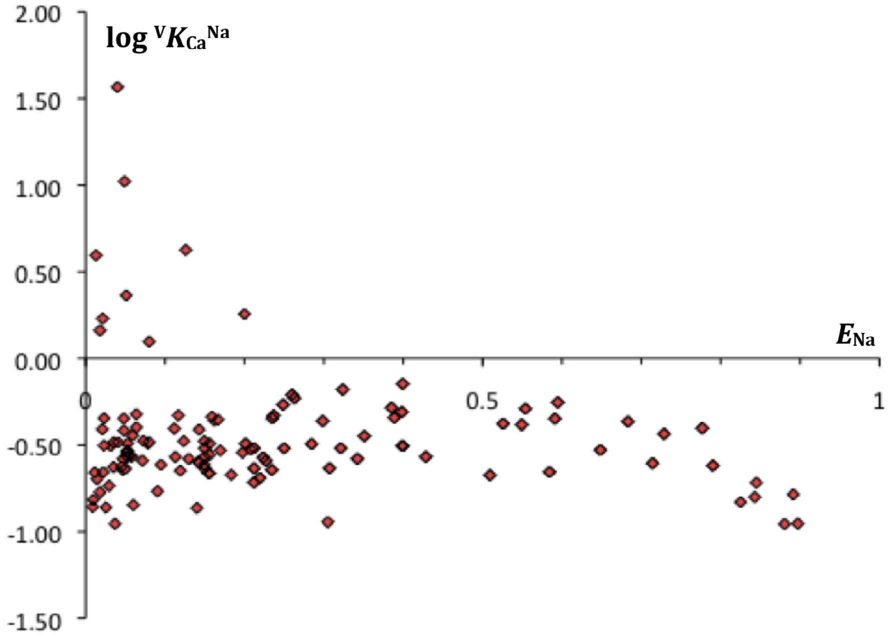

2.00
1.50
1.00
0.50
0.00
-0.50
-1.00
-1.50
0
0.5
1
log ${}^{V}K_{Ca}{}^{Na}$
E_{Na}

c.

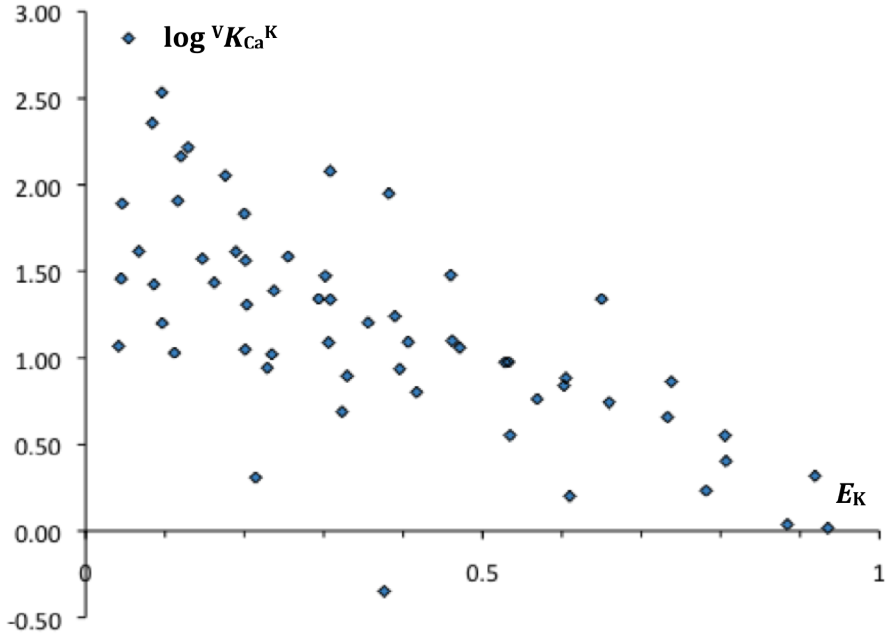

3.00
2.50
2.00
1.50
1.00
0.50
0.00
-0.50
0
0.5
1
log ${}^{V}K_{Ca}{}^{K}$
E_{K}

Figure 6.5 Conceptual model of the feedback between the ion exchange selectivity (^{V}K), population of exchangeable ions (E_i), and arrangement of clay particles (interlayer spacing, number of layers per stack) in smectite clay minerals (Laird and Shang, 1997).